MR and CT Evaluation of Intracranial Sarcoidosis

Wendelin S. Hayes, John L. Sherman, Barney J. Stern, Charles M. Citrin and Philip D. Pulaski

AJNR Am J Neuroradiol 1987, 8 (5) 841-847
http://www.ajnr.org/content/8/5/841

MR and CT Evaluation of Intracranial Sarcoidosis

Wendelin S. Hayes[1]
John L. Sherman[2, 3, 4]
Barney J. Stern[5, 6]
Charles M. Citrin[2, 3, 4]
Philip D. Pulaski[7, 8]

Fourteen patients with CNS manifestations of neurosarcoidosis were evaluated by MR imaging and CT. Evaluations were done on a 0.5-T superconductive magnet with T1- and T2-weighted sequences. CT with contrast was obtained in all patients. The granulomatous lesions were classified by location into basilar, convexity, intrahemispheric, and periventricular white-matter involvement. Hydrocephalus with or without an associated lesion was also noted. MR determined the presence of disease in all patients (100%), but was less accurate than CT in depicting disease in two patients (14%). CT determined the presence of disease in 12 patients (85%) and was less accurate than MR in delineating hypothalamic involvement in two patients and periventricular white-matter disease in three patients. There was great variability in the appearance of intracranial sarcoidosis on MR. Three patients had lesions that were isointense or hypointense (relative to cerebral cortex) on both T1- and T2-weighted images while nine patients had lesions that were hyperintense on T2-weighted images. Convexity involvement and hydrocephalus were well documented by both CT and MR.

These results indicate that both MR and CT are helpful in fully evaluating a patient with suspected intracranial sarcoidosis.

This article appears in the September/October 1987 issue of *AJNR* and the November 1987 issue of *AJR*.

Received December 12, 1986; accepted after revision April 16, 1987.

The opinions expressed herein are those of the authors and are not to be construed as reflecting the view of the Uniformed Services University of the Health Sciences or the Department of Defense.

[1] Department of Radiology, Georgetown University Hospital, Washington, DC 20007. Present address: Department of Radiology/Nuclear Medicine, Uniformed Services University of the Health Sciences, Bethesda, MD 20814-4799.

[2] Department of Radiology/Nuclear Medicine, Uniformed Services University of the Health Sciences, Bethesda, MD 20814-4799.

[3] Magnetic Imaging of Washington, 5550 Friendship Blvd., Chevy Chase, MD 20815. Address reprint requests to J. L. Sherman.

[4] Department of Radiology, George Washington University School of Medicine, Washington, DC 20037.

[5] Division of Neurology, Sinai Hospital, Baltimore, MD 21215.

[6] Department of Neurology, Johns Hopkins Hospital, Baltimore, MD 21205.

[7] Department of Neurology, George Washington University, School of Medicine, Washington, DC 20037.

[8] The Neurology Center, 5454 Wisconsin Ave., Chevy Chase, MD 21205.

***AJNR* 8:841–847, September/October 1987**
0195–6108/87/0805–0841

Neurologic manifestations of sarcoidosis occur in approximately 5% of patients with sarcoid [1–3]. Intracranial sarcoidosis may develop in a patient with known systemic disease or it may be the initial manifestation. Sarcoid granulomas have been found in the CNS and meninges in up to 14% of autopsy studies of patients with known sarcoidosis [4]. The CT characteristics of neurosarcoidosis have been well described [5–12], but there is limited information on the MR appearance of intracranial sarcoidosis [13]. In this study, we describe and compare the MR and CT appearance of CNS sarcoidosis.

Subjects and Methods

Fourteen patients with neurosarcoidosis underwent CT and MR examination of the brain. Most patients had biopsy-proven systemic sarcoidosis. Four of these patients had intracranial biopsies showing noncaseating granulomas. The diagnosis of neurosarcoidosis was made clinically in the 10 patients who did not undergo intracranial biopsy. In all of these cases, a clinical diagnosis of neurosarcoidosis of 2 to 10 years duration was present. There were eight women and six men ranging in age from 20 to 41 years.

All CT examinations were performed with IV contrast on third- or fourth-generation scanners. Thirteen patients had contrast-enhanced CT within 14 days of the MR study. One patient had her CT examination 2.5 months before the MR study.

All MR examinations were performed on a 0.5-T whole-body superconductive magnet (Vista-MR, Picker International, Highland Heights, OH). Standard, manufacturer-provided, single-echo spin-echo (SE) sequences were performed. Data were typically acquired with either 256 or 128 complex samples/view, 256 views, and four excitations using the two-dimensional Fourier transform method. A 256 × 256 or 128 × 256 matrix was employed. The field of view for these examinations was 23 or 25 cm. T2-weighted sequences were obtained using a TE of 60, 80, or 100 msec, and a TR of 1500–2500 msec. T1-weighted

TABLE 1: MR Characteristics in the Evaluation of Intracranial Sarcoidosis

Location/Type	Number	MR Signal Intensity (T2-Weighted Images)		
		(Hyper-)	(Hypo-)	(Iso-)
Basal	6	4	1	1
Periventricular	3	3	—	—
Convexity	2	1	1	—
Intracerebral lesion (hemispheric) mass	2	2	—	—
Hydrocephalus	3	1	—	2[a]
Total	16[b]	11	2	3

[a] MR determined the site of obstruction but the specific lesion could not be identified on MR.

[b] A total of 14 patients were studied. One patient had periventricular and basal involvement, and a second patient had basal involvement as well as an intracerebral mass lesion.

sequences employed a TE of 26–40 msec, with a TR of 500–800 msec. Sagittal T1-weighted images were obtained in all patients. The section thickness was 5 mm for all T1-weighted examinations. T2-weighted sequences were obtained with either 5-mm or 10-mm section thicknesses. The intensity of the lesions was compared with the intensity of cerebral cortex. The lesions were separated by location into basal, convexity, intracerebral (hemisphere), or periventricular involvement. Hydrocephalus with or without an associated lesion was also noted.

Results

The MR characteristics of the intracranial lesions are summarized in Table 1. Six patients had basilar lesions. Three of these six patients had subfrontal meningeal lesions and three had lesions that were in the region of the hypothalamus and suprasellar cistern. These latter patients had hypothalamic dysfunction clinically. Three patients had periventricular lesions and two patients had granulomatous involvement in the periaqueductal area. Two patients had involvement of the convexity (meningeal lesions). Two patients had hemispheric mass lesions, one lesion in the temporal lobe and one lesion in the parietal lobe.

MR detected basilar disease in six patients. In one patient who was on high-dose steroid therapy (dexamethasone 80 mg/day) at the time of both the CT and MR examinations, MR was not as effective as contrast-enhanced CT in detecting one basal lesion in the subfrontal region. MR examination in

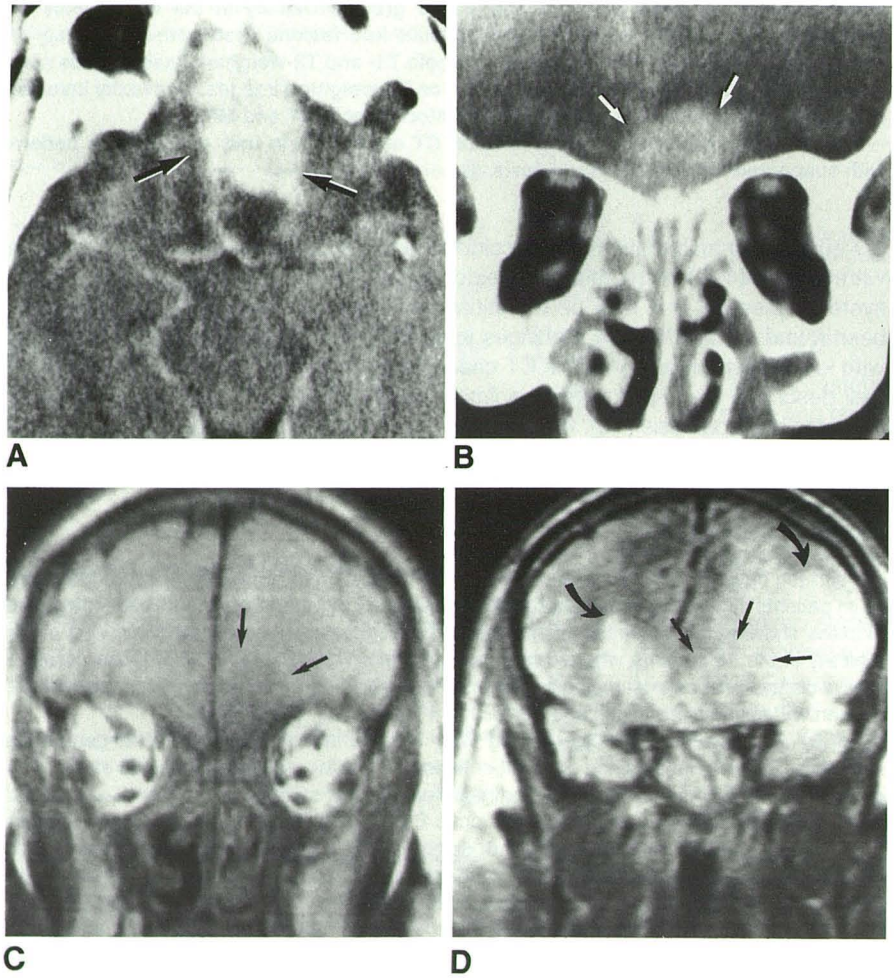

Fig. 1.—37-year-old man with subfrontal granulomatous involvement.

***A*, Contrast-enhanced axial CT. Homogeneously enhancing subfrontal mass (*arrows*).**

***B*, Contrast-enhanced coronal CT. Homogeneously enhancing granulomatous mass (*arrows*). Extensive sinus involvement (biopsy of sinus tissue showed sarcoid granuloma).**

***C*, T1-weighted coronal MR (SE 800/40). Left inferior frontal mass (*arrows*) isointense signal to cerebral cortex.**

***D*, T2-weighted coronal MR (SE 2000/60). Left inferior frontal lesion (*straight arrows*) isointense to cerebral cortex. Extensive edema of both frontal lobes (*curved arrows*).**

this patient showed subtle areas of increased signal in the subfrontal region on the T2-weighted images. The basilar involvement in another patient (not on high-dose steroid therapy) was isointense (relative to cerebral cortex) on both T1- and T2-weighted images (Fig. 1) with extensive edema of both frontal lobes surrounding the mass. In another patient, the lesion was hypointense on the T2-weighted images; this patient had involvement in the interhemispheric fissure from extension of basal meningeal granulomatous disease (Fig. 2). Three patients with hypothalamic and suprasellar cistern involvement had lesions of increased intensity on the T2-weighted image. One of these patients had undergone previous limited resection of a mass of granulomatous tissue in the temporal lobe. Changes in the temporal lobe could not be differentiated from postsurgical gliosis, but because the surgery was not extensive and subsequent MR revealed increased signal extending to the contralateral temporal lobe it seemed likely that the inflammatory process accounted for much of the MR appearance.

Enhanced CT detected abnormalities in all of the patients with basal involvement. Hypothalamic lesions in two patients were poorly seen on CT while one of these lesions was very prominent on MR (Fig. 3). The other hypothalamic lesion was detectable but poorly seen on both MR and CT.

Enhanced CT did not detect the periventricular white-matter lesions. The periventricular white-matter lesions in three patients were bright on the T2-weighted MR images. Extensive periventricular white-matter involvement seen on MR was an unexpected finding in one patient with suprasellar disease seen on contrast-enhanced CT (Fig. 4).

Two patients had convexity lesions seen well on both CT and MR. Both lesions were isointense relative to brain on the T1-weighted images. One lesion was heterogeneously hyperintense (Fig. 5) on the T2-weighted MR sections while the

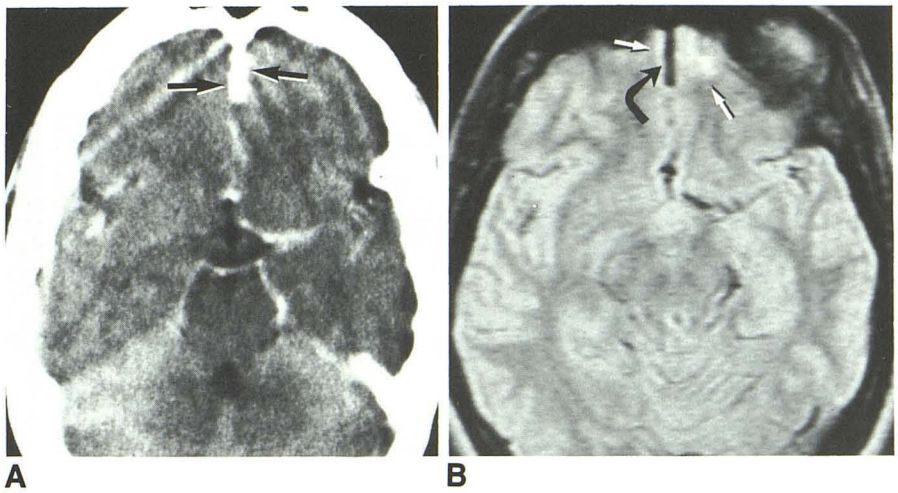

Fig. 2.—39-year-old woman with basal granulomatous (parafalcine) involvement.
***A*, Contrast-enhanced axial CT. Parafalcine enhancement (*arrows*). No calcification was noted in falx anteriorly on noncontrast CT.**
***B*, T2-weighted axial MR at same level as CT scan (SE 2500/60). Decreased signal along falx (*curved arrow*) with edema of adjacent cortex (*straight arrows*).**

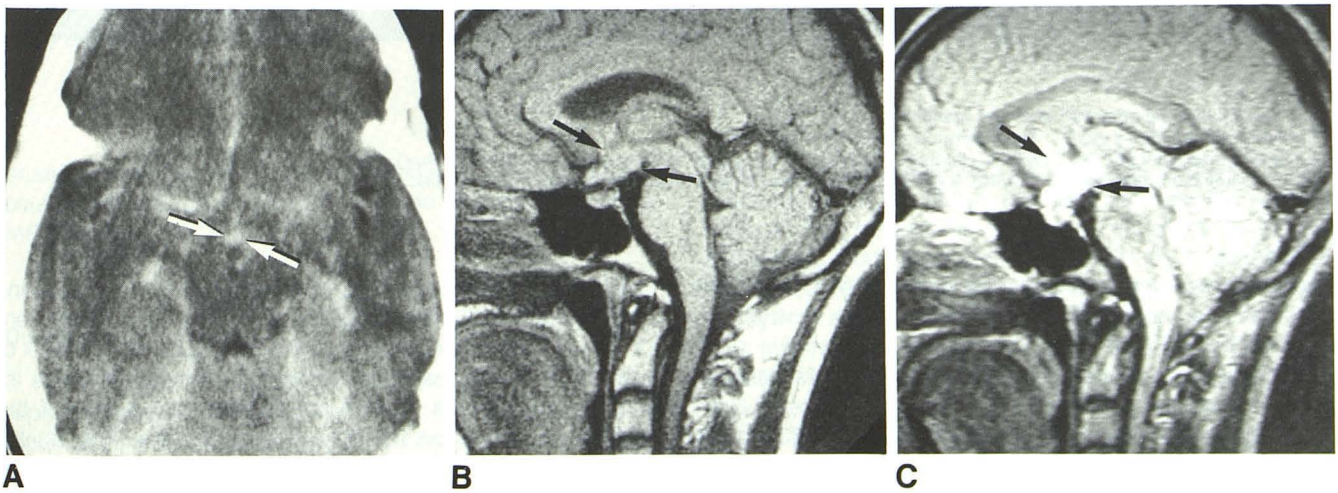

Fig. 3.—26-year-old woman with granulomatous involvement of hypothalamus.
***A*, Contrast-enhanced axial CT. Subtle enhancement in suprasellar area, midline (*arrows*), with obliteration of suprasellar cistern.**
***B*, T1-weighted sagittal MR (SE 550/40). Isointense mass in region of hypothalamus (*arrows*).**
***C*, T2-weighted sagittal MR (SE 1500/80). Increased signal in hypothalamic region (*arrows*).**

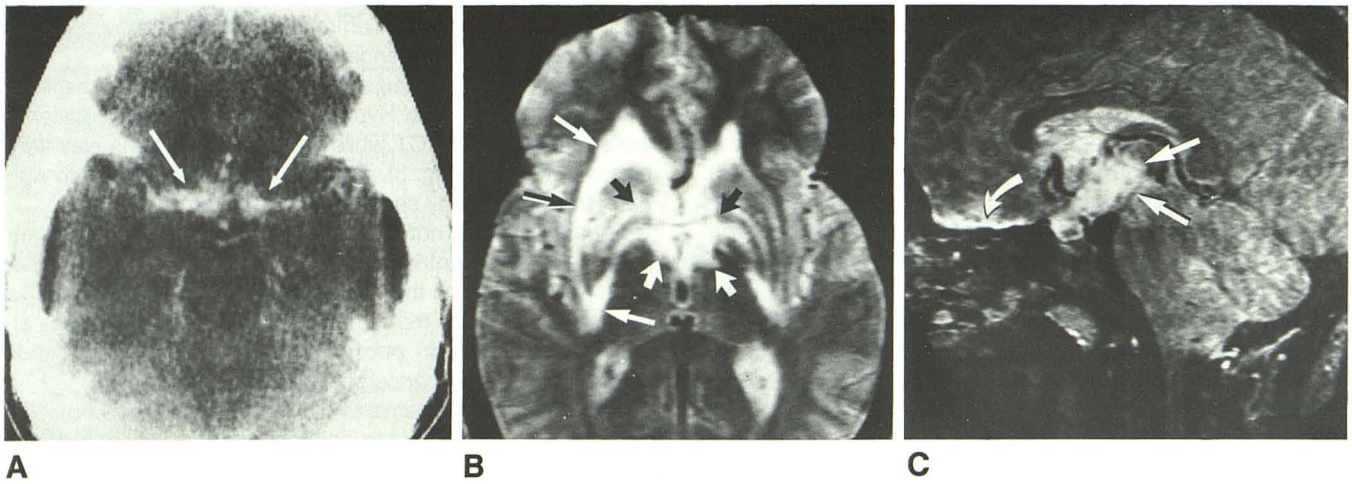

Fig. 4.—28-year-old man with suprasellar and periventricular white-matter disease.
***A*, Contrast-enhanced axial CT. Prominent enhancement in region of suprasellar cistern (*arrows*). Remainder of CT scan was unremarkable.**
***B*, T2-weighted axial MR (SE 2200/100). Increased signal showing basilar involvement including hypothalamus (*short arrows*). White-matter disease with increased signal involving periventricular region and internal and external capsule (*long arrows*).**
***C*, T2-weighted sagittal midline MR (SE 1600/100). Increased signal in hypothalamus (*straight arrows*) and subfrontal (basilar) region (*curved arrow*).**

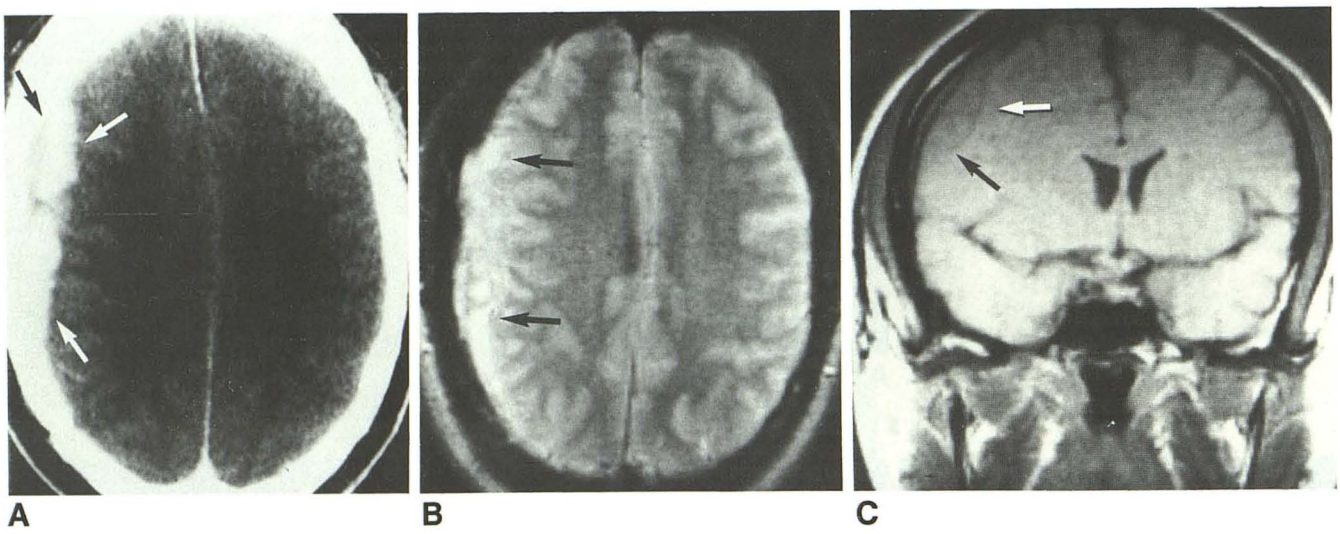

Fig. 5.—35-year-old man with subdural granuloma.
***A*, Contrast-enhanced axial CT. Enhancing extraaxial mass (*arrows*).**
***B*, T2-weighted axial MR (SE 3400/80). Heterogeneous increased signal of right extraaxial mass (*arrows*).**
***C*, T1-weighted coronal MR (SE 800/30). Right extraaxial mass (*arrows*) isointense with cerebral cortex.**

other lesion was predominantly hypointense (Fig. 6). These lesions showed homogeneous enhancement on contrast-enhanced CT.

Two patients had intracerebral (hemispheric) mass lesions, one in the parietal lobe and one in the temporal lobe. Both mass lesions were hyperintense on T2-weighted MR images and demonstrated homogeneous enhancement on contrast-enhanced CT.

One patient had hydrocephalus without a clearly identified obstructing lesion on MR or CT. The obstruction was at the level of the fourth ventricular outlet foramina (Fig. 7). MR showed no evidence of the CSF flow-void sign in the foramina of Magendie or Lushka despite ballooning of the fourth ventricle [14]. In another patient with hydrocephalus, the level of obstruction was the sylvian aqueduct, where abnormal increased signal was seen in the tectum at the level of the inferior aqueduct on the T2-weighted images (Fig. 8). No abnormal enhancement was seen on CT. There was interstitial edema surrounding the third and lateral ventricles. The aqueductal CSF flow-void sign was absent. The third patient with hydrocephalus who was on high-dose steroid therapy (prednisone 80 mg/day) at the time of both the CT and MR

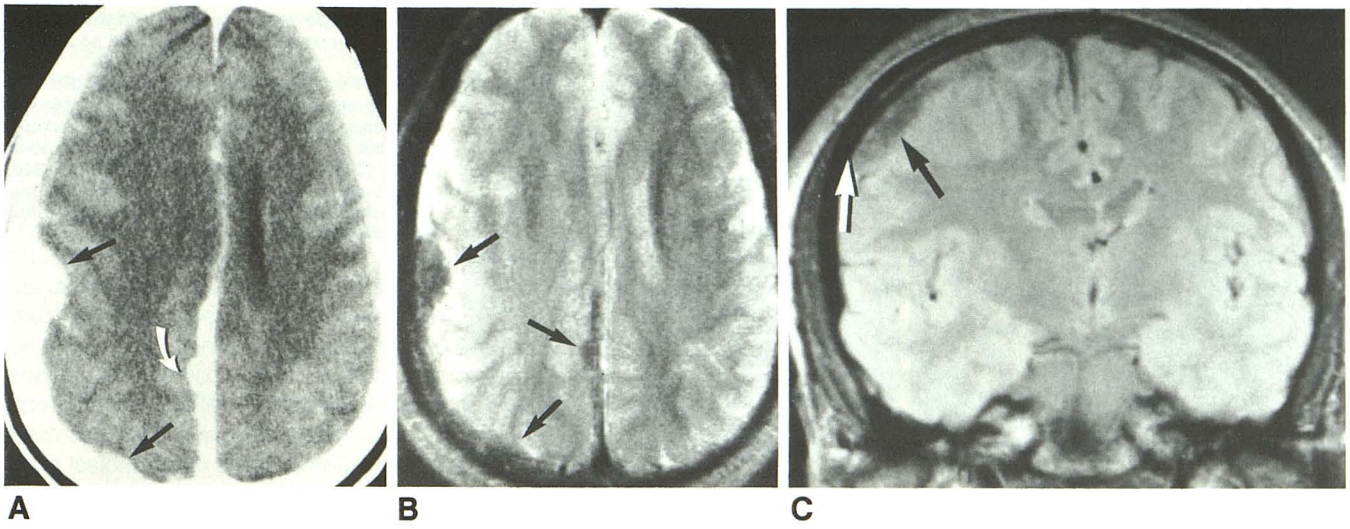

Fig. 6.—30-year-old man with extraaxial granulomatous mass.
***A*, Contrast-enhanced axial CT. Enhancing extraaxial mass (*straight arrows*). Note nodular extension posteriorly and in interhemispheric fissure (*curved arrow*).**
***B*, T2-weighted axial MR (SE 2500/60). Nodular extraaxial mass with interhemispheric extension hypointense relative to cerebral cortex (*arrows*).**
***C*, T2/T1 "balanced" coronal MR (SE 1200/40). Extraaxial mass slightly hypointense relative to cerebral cortex (*arrows*).**

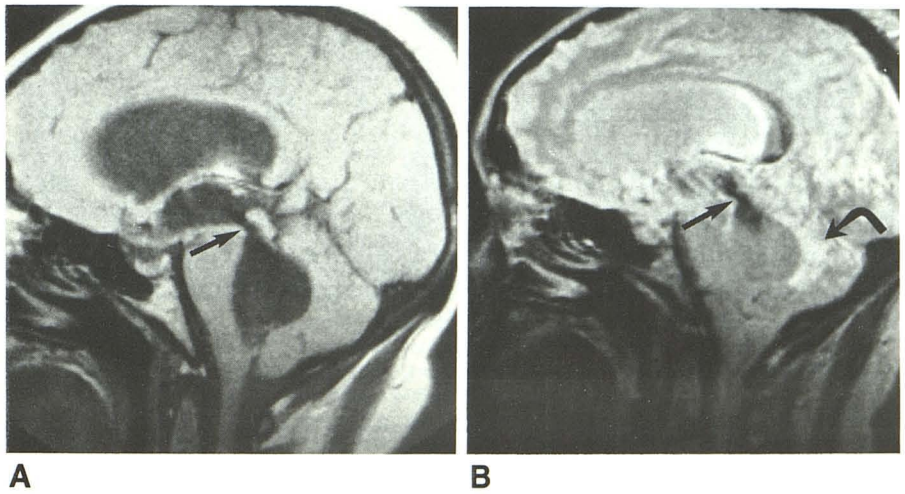

Fig. 7.—38-year-old woman with sarcoid-associated hydrocephalus and fourth-ventricular outlet obstruction.
***A*, T1-weighted midline sagittal MR (SE 700/40). Marked dilation of lateral, third, and fourth ventricles. CSF flow-void is seen in sylvian aqueduct (*arrow*).**
***B*, T2-weighted midline sagittal MR (SE 2000/60). Interstitial edema around fourth ventricle (*curved arrow*). CSF flow-void is seen in sylvian aqueduct (*straight arrow*) but is absent in caudal fourth ventricle.**

studies, demonstrated a contrast-enhancing lesion on CT causing aqueductal obstruction with no abnormal signal on MR (Fig. 9).

Discussion

The CNS manifestations of sarcoidosis include cranial neuropathies (any of the cranial nerves can be affected), aseptic meningitis, hydrocephalus, and parenchymatous disease [1–3, 15, 16]. Meningeal infiltration by granulomas is a common pathologic finding [2, 3, 6] and is clinically manifested as aseptic meningitis or extraaxial mass lesion.

Understanding of sarcoid-associated hydrocephalus and parenchymal disease is particularly important not only because imaging techniques are useful for diagnosis and assessment of clinical status, but also because the complications of CNS sarcoidosis account for much of the mortality and serious morbidity of the disease [17]. Hydrocephalus can be caused by periventricular inflammation, compression of the sylvian aqueduct [6] or fourth ventricle by mass lesions [18], inflammation involving the foramina of Lushka and Magendie [19], or inflammation and/or fibrosis of the subarachnoid space [2].

Parenchymatous disease [3, 5, 6, 8, 18] can cause an isolated mass of multiple nodules [9] in any part of the brain. Hypothalamic dysfunction is particularly common and may reflect the propensity of the granulomas to occur in the basal meninges [20]. A diffuse encephalopathy and vasculopathy is occasionally present and may represent widespread exten-

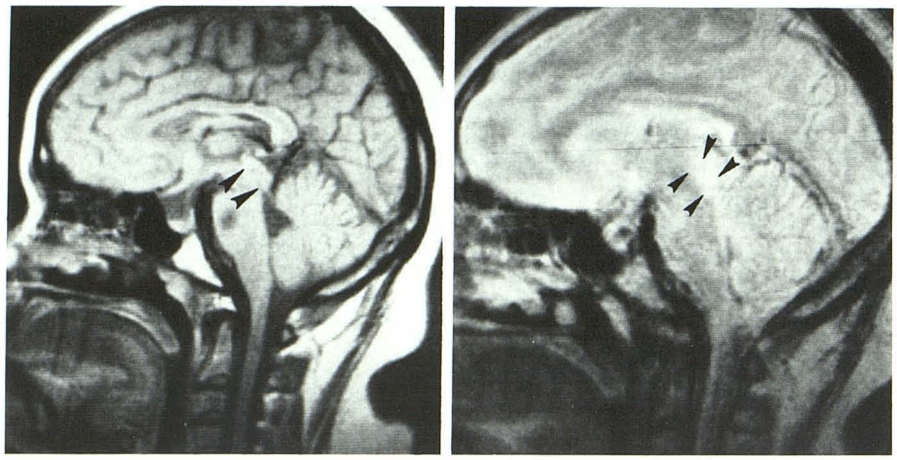

Fig. 8.—36-year-old woman with shunted sarcoid-associated hydrocephalus and aqueductal stenosis.

A, T1-weighted midline sagittal MR (SE 800/40), 5-mm section thickness. Postventricular-peritoneal shunt. Sylvian aqueduct is markedly stenotic (*arrows*). Note artifact in region of pons.

B, T2-weighted midline sagittal MR (SE 2400/80), 5-mm section thickness. Increased signal intensity around aqueduct (*arrows*) suggesting granulomatous involvement.

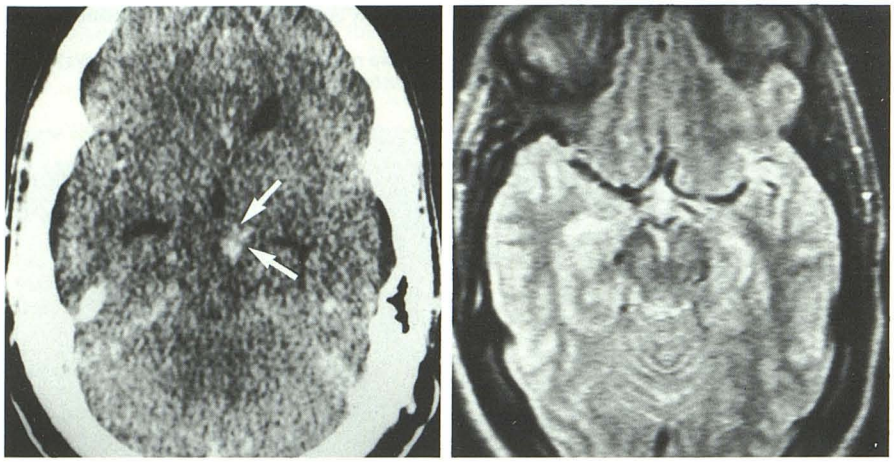

Fig. 9.—35-year-old woman with periaqueductal granulomatous lesion.

A, Contrast-enhanced axial CT. Enhancing left midbrain lesion (*arrows*) with compression of sylvian aqueduct and associated hydrocephalus.

B, T2-weighted axial MR (SE 2900/60). Section through tectum corresponds to level of CT (difference in slice angulation explains asymmetry at Circle of Willis). Lesion not identified on MR. Corresponding T1-weighted image was also unremarkable.

sion of meningeal inflammation along the Virchow-Robin spaces [21]. Seizures probably reflect cortical damage from the inflammatory process.

The CT appearance of neurosarcoidosis has been well documented [5–12, 17, 22, 23]. Hydrocephalus has been reported as the most common CT abnormality [3, 5, 6, 8] and was seen in only three of our 14 patients. With the advent of CT, intracranial mass lesions were more frequently seen [7] and may be asymptomatic. Granulomatous intracranial masses typically appear as well-defined, slightly hyperdense masses with varying degrees of edema on the noncontrast exam. These masses homogeneously enhance after contrast administration [5, 8, 9, 11, 18]. Intracranial mass lesions were identified by CT in 10 of our 14 patients. In all 10 patients, the lesions appeared to enhance. Marked white-matter edema has also been reported [11] and was present in one of our patients. Meningeal involvement may be seen as diffuse or focal enhancement of the meninges and underlying brain indistinguishable from meningeal carcinomatosis, fungal meningitis, or bacterial meningitis [24]. Masslike meningeal involvement may resemble an extensive en-plaque meningioma [25]. We observed meningeal enhancement in three of our patients. In patients with hydrocephalus, enhancement of the basal meninges on CT confirms the site of obstruction at the level of the base, and implies active inflammation rather than end-stage fibrosis [5]. Likewise, periventricular enhancement in hydrocephalic patients also suggests aggressive inflammation. An unusual infiltrative pattern of neurosarcoidosis on CT includes enhancing perivascular, linear, and nodular areas along the subarachnoid space extending into the white matter through the Virchow-Robin spaces [23].

Contrast-enhanced CT has been shown to be helpful in follow-up of patients with intracranial neurosarcoidosis on steroid therapy [5, 7, 8, 11, 22].

The CT findings demonstrated in our study correlated with the previously reported findings. A total of 11 intracranial mass lesions were seen, including two extraaxial dural granulomatous collections. Homogeneous enhancement of the

intracranial mass lesions on CT was demonstrated. Basilar enhancement (subfrontal meningeal lesions) reflecting active meningitis was seen on CT in three patients. Three patients demonstrated hydrocephalus on CT, but an enhancing periaqueductal mass was seen in only one of these patients.

In our comparative study of patients with known CNS sarcoidosis, there were two patients for whom MR was less accurate in depicting disease than was contrast-enhanced CT. Both these patients were on high-dose steroid therapy (dexamethasone 80 mg/day and prednisone 80 mg/day) at the time of both the CT and MR examinations. These findings on MR examination probably reflect the dramatic reduction in edema that can occur after the institution of steroids and the current unavailability of paramagnetic contrast agents. We have observed a similar phenomenon in other patients with brain lesions (such as metastatic tumors) after steroid treatment.

Five patients in our group had positive MR studies with either negative or subtly positive CT examinations. Two of these patients had hypothalamic lesions and three patients had periventricular white-matter disease.

Hydrocephalus was equally well seen with both CT and MR, but the associated periventricular white-matter edema was better detected with MR. Moreover, MR allowed evaluation of the CSF flow pattern by making visible the CSF flow-void sign [14]. MR was also particularly sensitive in detecting brainstem masses, the finding of which would encourage the clinician to treat the patient vigorously with antiinflammatory agents.

In summary, we often found that different, potentially complementary information was obtained by CT and MR. MR provided greater sensitivity than CT scanning in the evaluation of hypothalamic and periventricular involvement. The periventricular involvement on MR, as demonstrated in three of 14 patients, was a new and unexpected finding in CNS sarcoidosis. Hydrocephalus was better delineated on MR than on CT because the entire ventricular system could be evaluated. The sagittal presentation of MR images was preferable in these cases. CT was shown to be currently superior to MR in the evaluation of some patients on high-dose steroid therapy. We believe that both CT and MR are helpful for the full evaluation of patients with suspected CNS sarcoidosis.

ACKNOWLEDGMENT

The authors thank Martha Ross for manuscript preparation.

REFERENCES

1. Wiederholt WC, Siekert RG. Neurological manifestations of sarcoidosis. *Neurology* **1965**;15:1147–1154
2. Delany P. Neurological manifestation in sarcoidosis. Review of the literature with a report of 23 cases. *Ann Intern Med* **1977**;87:336–345
3. Stern BJ, Krumholz A, Johns C, Scott P, Nissim J. Sarcoidosis and its neurological manifestations. *Arch Neurol* **1985**;42:909–917
4. Ricker W, Clark M. Sarcoidosis: a clinical pathologic review of 300 cases, including 22 autopsies. *Am J Clin Path* **1949**;19:725–749
5. Kendall BE, Tatler GLV. Radiological findings in neurosarcoidosis. *Br J Radiol* **1978**;51:81–92
6. Kumpe DA, Krishna Rao CVG, Garcia JH, Heck AF. Intracranial neurosarcoidosis. *J Comput Assist Tomogr* **1979**;3:324–330
7. Brooks BS, El Gammal T, Hungerford GD. Radiological manifestations of neurosarcoidosis: role of computed tomography. *AJNR* **1982**;3:513–521
8. Bahr AL, Krumholz A, Kristt D, Hodges FJ. Neuroradiological manifestations of intracranial sarcoidosis. *Radiology* **1978**;127:713–717
9. Babu VS, Eisen H, Petaki K. Case report: sarcoidosis of the central nervous system. *J Comput Assist Tomogr* **1979**;3:396–397
10. Morehouse H, Danziger A. CT findings in intracranial neurosarcoid. *J Comput Tomogr* **1980**;4:267–270
11. Powers WJ, Miller EM. Sarcoidosis mimicking glioma: case report and review of intracranial sarcoid mass lesions. *Neurology* **1981**;31:907–910
12. Donovan Post MR, Quencer RM, Tabeli SZ. CT demonstration of sarcoidosis of the optic nerve, frontal lobes, and falx cerebri: case report and literature review. *AJNR* **1982**;3:523–526
13. Poole CJM. Argyll Robertson pupils due to neurosarcoidosis: evidence for site of lesion. *Br Med J* **1984**:289:356
14. Sherman JL, Citrin CM, Bowen BJ, Gangarosa RE. MR demonstration of altered CSF fluid flow by obstructive lesions. *AJNR* **1986**;7:571–579
15. Lawrence WP, El Gammal T, Pool WH Jr, Apter L. Radiological manifestations of neurosarcoidosis: report of three cases and review of literature. *Clin Radiol* **1974**;25:343–348
16. Silverstein A, Feuer MM, Siltzbach LE. Neurologic sarcoidosis: study of 18 cases. *Arch Neurol* **1965**;12:1–11
17. Luke RA, Stern BJ, Krumholz A, Johns CK. Neurosarcoidosis: the long-term clinical course. *Neurology* (in press)
18. Whelan MA, Stern J. Sarcoidosis presenting as a posterior fossa mass. *Surg Neurol* **1981**;15:455–457
19. Lukin RR, Chambers AA, Soleimanpour M. Outlet obstruction of the fourth ventricle in sarcoidosis. *Neuroradiology* **1975**;10:65–68
20. Brust JCM, Rhee RS, Plank CR, Newmark M, Felton CP, Lewis LD. Sarcoidosis, galactorrhea, and amenorrhea: two autopsy cases, one with Chiari-Frommel syndrome. *Ann Neurol* **1977**;2:130–137
21. Herring AB, Urich H. Sarcoidosis of the central nervous system. *J Neurol Sci* **1969**;9:405–422
22. Healton EB, Zito G, Chauhan P, Brust JCM. Intracranial subdural sarcoid granuloma. *J Neurosurg* **1982**;56:728–731
23. Mirfakhraee M, Crofford MJ, Guinto FC, Nauta HJW, Weedn VW. Virchow-Robin space: a path of spread in neurosarcoidosis. *Radiology* **1986**;158:715–720
24. Enzmann DR, Norman D, Mani J, Newton TH. Computed tomography of granulomatous basal arachnoiditis. *Radiology* **1976**;120:341–344
25. Osenbach RK, Blumenkopf B, Ramirez H, Gutierrez J. Meningeal neurosarcoidosis mimicking convexity en-plaque meningioma. *Surg Neurol* **1986**;26:387–390